MCB
Journals.ASM.org

The E3 Ubiquitin Ligase ARIH1 Protects against Genotoxic Stress by Initiating a 4EHP-Mediated mRNA Translation Arrest

Louise von Stechow,[a] Dimitris Typas,[b] Jordi Carreras Puigvert,[a,b] Laurens Oort,[a] Ramakrishnaiah Siddappa,[a] Alex Pines,[b] Harry Vrieling,[b] Bob van de Water,[a] Leon H. F. Mullenders,[b] Erik H. J. Danen[a]

Division of Toxicology, Leiden/Amsterdam Center for Drug Research, Leiden University, Leiden, The Netherlands[a]; Department of Toxicogenetics, Leiden University Medical Center, Leiden, The Netherlands[b]

DNA damage response signaling is crucial for genome maintenance in all organisms and is corrupted in cancer. In an RNA interference (RNAi) screen for (de)ubiquitinases and sumoylases modulating the apoptotic response of embryonic stem (ES) cells to DNA damage, we identified the E3 ubiquitin ligase/ISGylase, ariadne homologue 1 (ARIH1). Silencing ARIH1 sensitized ES and cancer cells to genotoxic compounds and ionizing radiation, irrespective of their p53 or caspase-3 status. Expression of wild-type but not ubiquitinase-defective ARIH1 constructs prevented sensitization caused by ARIH1 knockdown. ARIH1 protein abundance increased after DNA damage through attenuation of proteasomal degradation that required ATM signaling. Accumulated ARIH1 associated with 4EHP, and in turn, this competitive inhibitor of the eukaryotic translation initiation factor 4E (eIF4E) underwent increased nondegradative ubiquitination upon DNA damage. Genotoxic stress led to an enrichment of ARIH1 in perinuclear, ribosome-containing regions and triggered 4EHP association with the mRNA 5′ cap as well as mRNA translation arrest in an ARIH1-dependent manner. Finally, restoration of DNA damage-induced translation arrest in ARIH1-depleted cells by means of an eIF2 inhibitor was sufficient to reinstate resistance to genotoxic stress. These findings identify ARIH1 as a potent mediator of DNA damage-induced translation arrest that protects stem and cancer cells against genotoxic stress.

DNA damage leads to acute toxicity and the accumulation of mutations and chromosomal instability, potentially resulting in malignant transformation (1, 2). To counteract these deleterious effects of DNA damage, the cell is equipped with a highly complex signaling response termed the DNA damage response (DDR). The DDR activates effector components involved in protective pathways, including DNA damage repair, cell cycle arrest, transcription regulation, chromatin remodeling, and cell death (1). The complex of DDR signaling pathways is crucial for the protection of the genome in all organisms. Moreover, understanding DDR signaling in the context of chemical or ionizing radiation-induced DNA damage is important to design improved strategies to combat therapy resistance. In tandem with phosphorylation-mediated signaling, which is largely executed by the phosphoinositol 3-kinase (PI3K)-like kinases ATM, ATR, and DNA-dependent protein kinase (DNA-PK), the checkpoint kinases Chk1 and Chk2, and members of the mitogen-activated protein kinase (MAPK) family (3, 4), protein modifications by ubiquitin and ubiquitin-like moieties are crucial at all levels of the DDR (5).

The ubiquitination machinery can form various, differentially interpreted tags, including both degradative (K48- and K11-linked chains) and nondegradative (monoubiquitination and K63-linked chains) signals (6). Furthermore, a growing family of ubiquitin-like modifications, such as SUMO, Nedd8, and ISG15, has been identified, mostly providing nondegradative signals. Multiple enzymes are shared between the ubiquitination, sumoylation, and ISGylation systems (7–9). Ubiquitin-mediated signaling is vital to many cellular processes, including the response to DNA damage. Recognition and processing of double-strand breaks (DSBs) and intrastrand cross-links, polymerase switching during translesion synthesis (TLS), nucleotide excision repair, and p53 stability are all regulated by ubiquitination (5, 10, 11). More recently, ISGylation has been implicated in the DDR: ATM-mediated downmodulation of the ISG system can serve as a mechanism to enhance ubiquitination-mediated protein turnover after DNA damage (12).

Ubiquitin and ubiquitin-like modifications occur through three enzymatic steps, commencing with an E1 activating enzyme, which forms a thioester bond to the ubiquitin protein. Subsequently, the charged ubiquitin monomer is relayed to an E2 enzyme that conjugates the ubiquitin molecule to its target protein with the aid of an E3 ubiquitin ligase (13). While there are only a few E1 and E2 enzymes, a large number of E3 ubiquitin ligases dictates substrate specificity and ensures substrate diversity of the ubiquitin system (13). There are two E3 ubiquitin ligase families. In RING ubiquitinases, the ligase functions as an adaptor between the E2 enzyme and the substrate, facilitating transfer of the ubiquitin moiety to the target protein. In HECT ubiquitinases, the ubiquitin is first conferred on a conserved residue within the HECT domain and then added to the substrate protein (14). Recently, ubiquitin ligases of the parkin family, including parkin and

Received 12 September 2014 **Returned for modification** 30 September 2014
Accepted 16 January 2015

Accepted manuscript posted online 26 January 2015

Citation von Stechow L, Typas D, Carreras Puigvert J, Oort L, Siddappa R, Pines A, Vrieling H, van de Water B, Mullenders LHF, Danen EHJ. 2015. The E3 ubiquitin ligase ARIH1 protects against genotoxic stress by initiating a 4EHP-mediated mRNA translation arrest. Mol Cell Biol 35:1254–1268. doi:10.1128/MCB.01152-14.

Address correspondence to Leon H. F. Mullenders, l.mullenders@lumc.nl, or Erik H. J. Danen, e.danen@lacdr.leidenuniv.nl.

L.V.S. and D.T. contributed equally to this article.

Supplemental material for this article may be found at http://dx.doi.org/10.1128/MCB.01152-14.

doi:10.1128/MCB.01152-14

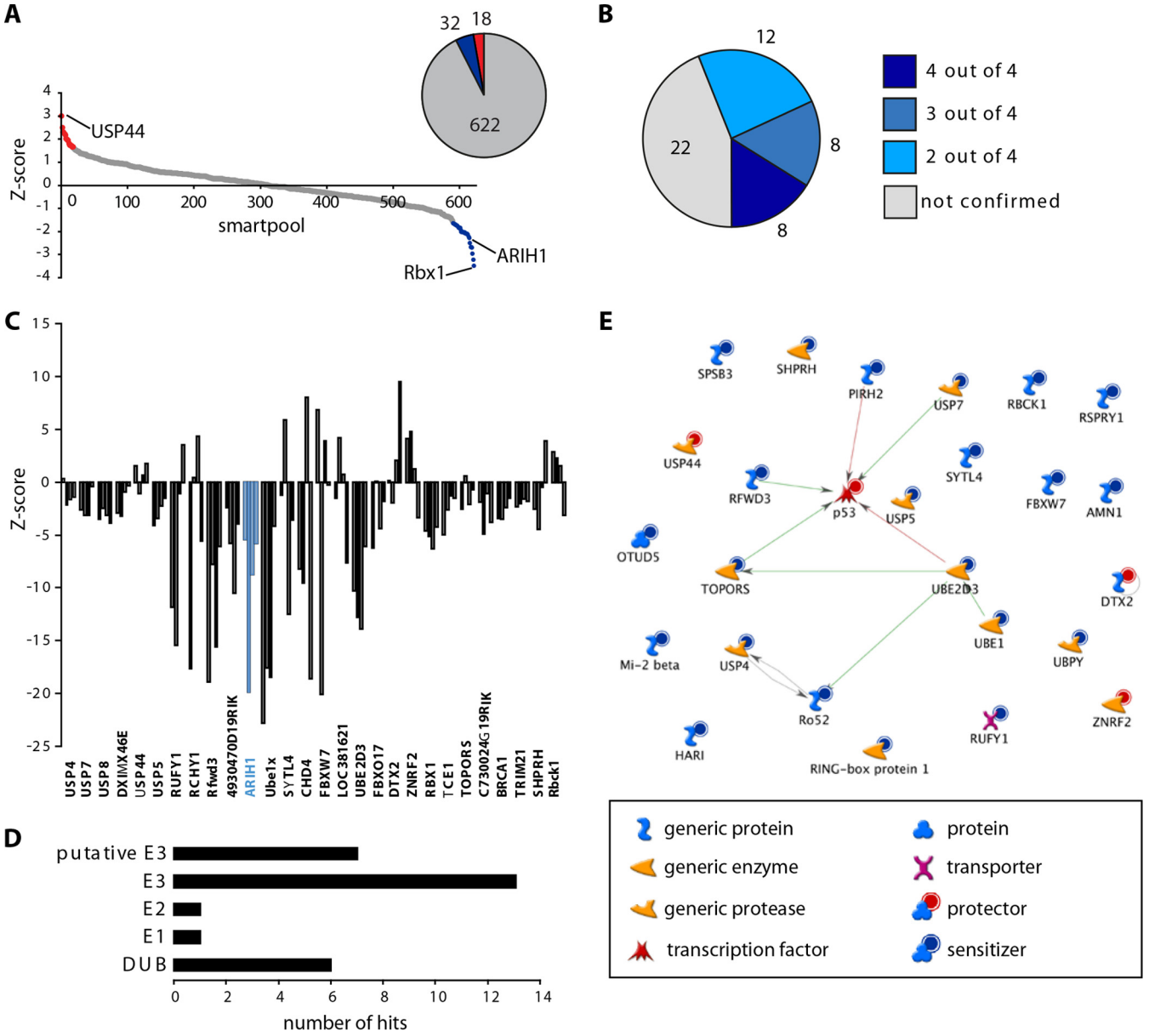

FIG 1 RNAi screen for ubiquitination/sumoylation enzymes identifies CP response modulators. (A) Hits identified in primary screens; protecting siRNA SMARTpools are in red, and sensitizing siRNA SMARTpools are in blue. (B) Results of deconvolution screen for 50 SMARTpools identified in primary screen. (C) Z-scores obtained for 28 confirmed hits in deconvolution screen. ARIH1 results are in blue. (D) Distribution of hits over different gene families as indicated. (E) Metacore-predicted network derived from screen hits; interactions with p53 are indicated. protector, protecting siRNAs; sensitizer, sensitizing siRNAs.

human homologue of ariadne 1 (ARIH1; HHARI), have been demonstrated to be hybrids between HECT and RING domain ubiquitin ligases (15).

In response to DNA damage, ongoing transcription and translation have to be adjusted to allow execution of stress-specific programs, save energy, accomplish DNA repair, and avoid the transcription and subsequent translation of potentially mutated genetic material (16). Genotoxic stress has been shown to induce a block in protein synthesis (17–19). Eukaryotic mRNAs are mostly recruited to the ribosome through their 5′ 7-methylguanosine cap (20). The rate-limiting step of eukaryotic cap-dependent translation initiation is the binding of the eukaryotic initiation factor 4F (eIF4F) complex to the mRNA 5′ cap structure. eIF4F is composed of the cap-binding protein, eIF4E, the RNA helicase eIF4A, and the scaffold protein eIF4G (21, 22). Recruitment of additional eIF proteins and the 40S ribosomal subunit completes the preinitiation complex that scans the mRNA for the AUG codon and drives mRNA translation initiation (20–22). If eIF4E is replaced by its structural analogue, 4EHP, at the mRNA 5′ cap, this prevents formation of the preinitiation complex (20). Thus, 4EHP constitutes a negative regulator of translation initiation.

Here, we describe the identification of the parkin family E3 ubiquitin ligase ARIH1 in an RNA interference (RNAi) screen for modulators of chemosensitivity. We show that ARIH1 levels and

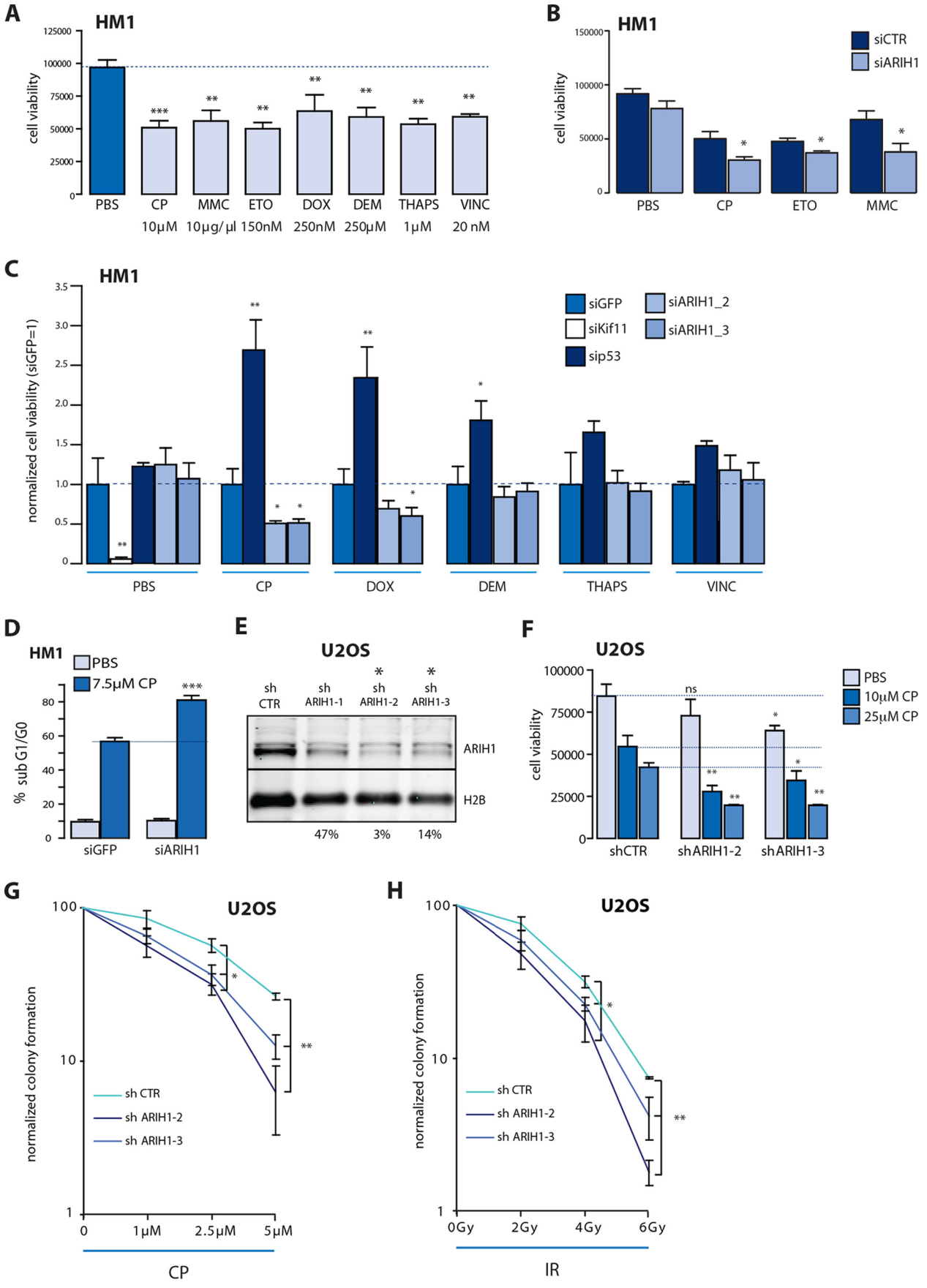
A
HM1
cell viability
125000
100000
75000
50000
25000
0
PBS
CP
10μM
MMC
10μg/μl
ETO
150nM
DOX
250nM
DEM
250μM
THAPS
1μM
VINC
20 nM
B
HM1
siCTR
siARIH1
cell viability
150000
100000
50000
0
PBS
CP
ETO
MMC
C
HM1
normalized cell viability (siGFP=1)
siGFP
siKif11
sip53
siARIH1_2
siARIH1_3
PBS
CP
DOX
DEM
THAPS
VINC
D
HM1
PBS
7.5μM CP
% sub G1/G0
siGFP
siARIH1
E
U2OS
sh CTR
sh ARIH1-1
sh ARIH1-2
sh ARIH1-3
ARIH1
H2B
47%
3%
14%
F
U2OS
cell viability
PBS
10μM CP
25μM CP
ns
shCTR
shARIH1-2
shARIH1-3
G
U2OS
normalized colony formation
sh CTR
sh ARIH1-2
sh ARIH1-3
0
1μM
2.5μM
5μM
CP
H
U2OS
normalized colony formation
sh CTR
sh ARIH1-2
sh ARIH1-3
0Gy
2Gy
4Gy
6Gy
IR

cellular localization are regulated in response to DNA damage. In turn, ARIH1 protects stem and cancer cells against genotoxic compounds and gamma irradiation (IR) by promoting and fine-tuning a 4EHP-mediated mRNA translation arrest.

MATERIALS AND METHODS

Cell culture, plasmids, and other reagents. HM1 mouse embryonic stem (ES) cells derived from an OLA/129 genetic background (provided by Klaus Willecke, University of Bonn) were maintained under feeder-free conditions in Glagow minimum essential medium containing 5×10^5 U of mouse recombinant leukemia inhibitory factor (LIF; PAA). All other cell lines were purchased from the ATCC. MCF7 human breast cancer cells and H1299 human non-small-cell lung cancer cells were maintained in RPMI medium. U2OS human sarcoma cells were kept in Dulbecco modified Eagle medium (DMEM). All media contained 10% fetal bovine serum (FBS), 25 U/ml of penicillin, and 25 μg/ml of streptomycin. All cell lines, including stable short hairpin RNA (shRNA)-expressing derivatives, were confirmed to be mycoplasma free using the Mycosensor kit from Stratagene.

Wild-type (17342) and non-ISGylatable (K121/130/134/222R [4KR]) mutant (17353) FLAG-tagged versions of 4EHP, as well as hemagglutinin (HA)-tagged ISG15 (12444), were provided by Dong-Er Zhang, Scripps Research Institute, La Jolla, CA, through Addgene (23). By means of site-directed mutagenesis, a point mutation (C208A) was introduced into wild-type ARIH1 cDNA, yielding an ubiquitination-deficient ARIH1 mutant (24). Wild-type and C208A ARIH1 cDNAs were cloned into entry vector pENTR4-GFP-C1 (w392-1), provided by E. Campeau, University of Massachusetts Medical School, Worcester, MA, through Addgene (25). Subsequently, they were recombined into pLenti6.3 V5-DEST (Invitrogen) using Gateway recombination. Destination vectors containing such green fluorescent protein (GFP)-tagged ARIH1 versions were used for either direct overexpression in mammalian cells or lentiviral production.

Genotoxicants included the DNA cross-linkers cisplatin [CP; *cis*-$PtCl_2(NH_3)_2$] (provided by the Pharmacy Unit of University Hospital, Leiden, The Netherlands) and mitomycin C (Sigma), as well as the inhibitors of topoisomerase II-mediated DNA unwinding doxorubicin (Sigma) and etoposide (Sigma). The oxidative stressor diethyl maleate (DEM), the microtubule poison vincristine, and the endoplasmic reticulum (ER) stressor thapsigargin were from Sigma. The pan-caspase inhibitor z-Val-Ala-DL-Asp-fluoromethylketone (z-VAD-fmk) was purchased from Bachem, and the eIF2α dephosphorylation inhibitor salubrinal was from Calbiochem. The ATM inhibitor KU-5593 and proteasome inhibitor MG132 were from Tocris Biosciences. Antibodies against p53 and phospho-p53(Ser15) were purchased from Novacostra and Cell Signaling, respectively. Antibodies against tubulin and FLAG were obtained from Sigma. Antibodies against mouse or human 4EHP and eIF4G2 were from Cell Signaling. ARIH1 antibody was from Novus Biologicals. Monoclonal antibody against ubiquitin was purchased from Enzo Biochem (FK2 clone).

RNAi experiments. Small interfering RNAs (siRNAs) were purchased from ThermoFisher Scientific. For primary screens, the Dharmacon siGENOME SMARTpool siRNA Library—mouse ubiquitin conjugation subsets 1 (G-015610), 2 (G-015620), and 3 (G-015630)—were used. For deubiquitination and SUMOylation screens, customized siGENOME SMARTpool siRNA libraries were used (see Table S1 in the supplemental material). For deconvolution confirmation screens, customized libraries containing 4 individual siRNAs targeting each selected mRNA were used. GFP, lamin A/C, and RISC-free control siRNAs were used according to minimum information about an RNAi experiment (MIARE) guidelines. Kif11 siRNA was used as transfection efficiency control.

The siRNA screens were performed on a Biomek FX (Beckman Coulter) liquid handling system. A 50 nM concentration of siRNA was transfected in 96-well plates using Dharmafect1 transfection reagent (ThermoFisher Scientific). The medium was refreshed every 24 h, and cells were exposed to indicated compounds or vehicle controls at 64 h posttransfection for 24 h. Primary screens were done in duplicate, and deconvolution screens were done in quadruplicate. As readout, a cell viability assay using ATPlite 1Step kit (PerkinElmer) was performed according to the manufacturer's instructions, followed by luminescence measurement using a plate reader.

For stable gene silencing, cells were transduced using lentiviral TRC shRNA vectors at a multiplicity of infection (MOI) of 1 (LentiExpress; Sigma-Aldrich; Rob Hoeben and Martijn Rabelink, University Hospital, Leiden, The Netherlands) according to the manufacturer's procedures and bulk selected in medium containing 2.5 μg/ml of puromycin. Control vector expressed shRNA targeting TurboGFP. shRNAs targeting ARIH1 were CCAGATGAATACAAGGTCATC (shARIH1-1), CTACCTTGAAC GAGATATTTC (shARIH1-2), and CTGTTAAATGTAAGTGGTTAC (shARIH1-3).

For ARIH1 gene silencing in combination with ectopic expression of GFP-ARIH1 constructs, an siRNA targeting the 3′ untranslated region (UTR) (GCACACAGCUGUAGGCAUUUU) of ARIH1 was used (ThermoFisher Scientific).

RNAi screen data analysis. As a quality control, Z′ factors were determined for each plate, using lamin A/C as a negative control and p53 as a positive control. To rank the results, Z-scores were calculated using as a reference (i) the mean of all test samples in the primary screen and (ii) the mean of the negative-control samples in the secondary deconvolution screen (in order to prevent bias due to preenrichment of hits) (26). Hit determination was done using Z-scores with a cutoff value of 1.5 below or above the reference and a *P* value lower than 0.05. Enrichment of canonical pathways and formation of the p53/ubiquitination signaling network was performed using MetaCore data mining software.

Apoptosis and cell cycle analysis. ES cells were exposed to a vehicle or CP for 8 h for cell cycle analysis or 24 h for apoptosis analysis. MCF7 cells were exposed for 24 h for cell cycle analysis. Floating and attached cells were pooled and fixed in 80% ethanol overnight. Cells were stained using phosphate-buffered saline (PBS)-EDTA containing 7.5 mM propidium

FIG 2 Silencing ARIH1 sensitizes to genotoxic stress. (A) ES cell viability after treatment for 24 h with the indicated equitoxic concentrations of CP, mitomycin C (MMC), etoposide (ETO), doxorubicin (DOX), diethyl maleate (DEM), thapsigargin (THAPS), or vincristine (VINC). (B) ES cell viability in the presence of control (CTR) or ARIH1 siRNA after treatment with equitoxic concentrations of CP, ETO, or MMC. (C) ES cell viability in the presence of Kif11-siRNA (only for PBS), GFP-siRNA, p53-siRNA, or 2 individual siRNA sequences targeting ARIH1 after treatment with equitoxic concentrations of CP, DOX, DEM, THAPS, or VINC (normalized to siGFP). (D) Sub-G_0/G_1 apoptotic fraction of control or siARIH1 ES cells treated with 7.5 μM CP for 24 h. (E) ARIH1 protein levels and H2B loading control in U2OS cells bulk puromycin selected for expression of sh-control or 3 individual shRNAs targeting ARIH1. Percentages indicate remaining ARIH1 expression. Asterisks indicate shARIH1-2 and shARIH1-3, used in all further experiments. (F) U2OS cell viability in sh-control or 2 individual shARIH1 cell lines after treatment with a vehicle (PBS) or 10 or 25 μM CP for 48 h. Raw values of luminescence for treatment with PBS and with 10 and 25 μM CP (means ± SEMs) were as follows: for sh-control, 84,534 ± 8,398, 54,502 ± 6,677, and 42,276 ± 1,720, respectively; for shARIH1-2, 72,869 ± 11,532, 27,894 ± 3,564, and 19,722 ± 258, respectively; and for shARIH1-3, 64,028 ± 3,582, 34,457 ± 5,661, and 19,682 ± 273, respectively. (G) Colony formation capacity in sh-control or shARIH1-2 and -3 U2OS cell lines after 24 h treatment with CP at the indicated concentrations. Nonnormalized means ± SDs for 0, 1, 2.5, and 5 μM CP were as follows: for sh-control, 79.67 ± 7.79, 81.00 ± 13.55, 43.67 ± 3.89, and 23.00 ± 3.54, respectively; for shARIH1-2, 65.33 ± 5.49, 39.33 ± 4.71, 22.67 ± 3.89, and 5.00 ± 1.63, respectively; and for shARIH1-3, 56.67 ± 2.48, 40.33 ± 4.26, 24.67 ± 5.93, and 9.00 ±1.22, respectively. (H) Colony formation capacity in sh-control or shARIH1-2 and -3 U2OS cell lines after 24 h of treatment with the indicated IR doses. *, $P < 0.05$; **, $P < 0.01$; ***, $P < 0.001$ (Student's *t* test).

iodine and 40 mg/ml of RNase A and measured by flow cytometry (FACSCanto II; Becton Dickinson). The amounts of cells in the different cell cycle fractions or in sub-G_0/G_1 for apoptotic cells were calculated using BD FACSDiva software. Alternatively, apoptosis was determined using live imaging of annexin V labeling, as described previously (27).

Clonogenic survival assay. U2OS cells (250 cells/plate) expressing different shRNAs were seeded in triplicate in 9-cm plates. The following day, cells were treated for 24 h with a dose range of CP or IR. After a recovery period of 10 days, surviving cells were fixed and stained and colonies were counted to assay each cell line's clonogenic potential.

Western blot analysis. Extracts were prepared in Tris-sucrose-EDTA buffer containing protein inhibitor cocktail, separated by SDS-PAGE on polyacrylamide gels, and transferred to polyvinylidene difluoride (PVDF) membranes; membranes were blocked using 5% bovine serum albumin (BSA). Following incubation with primary and secondary antibodies, signal was detected using a Typhoon 9400 from GE Healthcare.

Immunofluorescence. U2OS cells were seeded on glass coverslips and allowed to grow for 2 days. Subsequently, they were treated with CP and fixed using 2% formaldehyde for 20 min at the desired time points. After extensive washing and rehydration in PBS, postfixation extraction took place by incubation with 0.25% Triton X-100 for 5 min. Cells were extensively washed with PBS to remove detergent and then blocked in 5% BSA. Finally, coverslips were immunostained with mouse anti-FLAG and rabbit anti-eiF4G2 antibodies and appropriate secondary fluorescent antibodies.

Cap binding assay. HM1 ES cells, U2OS cells, and MCF7 breast cancer cells were seeded in 6-well plates at a density of 0.5 million cells/well. Cells were treated with different concentrations of CP for 4 h (U2OS and MCF7) or 8 h (ES), and proteins were harvested in lysis buffer containing 1 mM phenylmethylsulfonyl fluoride (PMSF; Cell Signaling). Cap binding proteins were precipitated using 7-methyl-GTP–Sepharose 4B beads (Amersham) as described previously (28). Precipitated proteins were separated on 12% SDS-PAGE gels and analyzed by immunoblotting for 4EHP (eIF4E2).

Metabolic labeling for detection of translational changes after CP treatment. Click-iT metabolic labeling reagents for proteins were purchased from Invitrogen and used according to the manufacturer's instructions. In short, U2OS cells were seeded to 80% confluence in 96-well μclear plates and subsequently treated with 15 μM CP for 2 to 8 h or with 2 mg/ml of cycloheximide (CHX) for 1 h, or for 2 h with a combination of 15 μM CP and 2.5 μM salubrinal. During the last hour of treatment, medium was replaced with methionine-free medium. Subsequently, cells were incubated with azide-labeled methionine analogue for 1 h, fixed for 15 min in 4% formaldehyde, and stained according to the manufacturer's protocol. 4′,6-Diamidino-2-phenylindole (DAPI) was used as a counterstain, and images were acquired using a BD-pathway imaging system. Image analysis was performed using BD Attovision software.

FLAG coimmunoprecipitation. U2OS cells, expressing different shRNAs, were transiently transfected with FLAG-tagged wild-type 4EHP or K121/130/134/222R (4KR) mutant 4EHP cDNAs or FLAG-LacR control plasmid in absence or presence of pCAGGS-5HA-mISG15 cDNA in Opti-MEM (Invitrogen), using JetPEI (Polyplus Transfection). The following day, the medium was refreshed, and 48 h posttransfection, cells were lysed in FLAG lysis buffer (50 mM Tris-HCl [pH 7.4], 150 mM NaCl, 1 mM EDTA, 0.5% NP-40, 0.5% Triton X-100, and 1 mM PMSF, supplemented with complete protease inhibitor cocktail [Roche]). After 30 min of incubation on ice, lysates were diluted 5 times with FLAG dilution buffer (50 mM Tris-HCl [pH 7.4], 150 mM NaCl, 1 mM EDTA, and 1 mM PMSF, supplemented with complete protease inhibitor cocktail) and incubated with prewashed M2-FLAG magnetic beads (Sigma) for 3 h. Subsequently, beads were washed 3 times for 5 min with FLAG dilution buffer and lysed in Laemmli-SDS sample buffer. FLAG-ARIH1 coimmunoprecipitation from lysates from SILAC-labeled (where SILAC stands for stable isotope labeling of cells in culture) cells followed by mass spectrometry (MS) was performed as described above, with the exception of eluting FLAG-bound proteins by competition with the 3× FLAG peptide instead of boiling in sample buffer. Following elution, samples were trypsinized overnight, desalted, freeze-dried, and finally used for MS analysis.

qPCR. RNA was extracted using RNeasy Plus minikit from Qiagen. cDNA was made from 50 ng of total RNA with a RevertAid H minus first-strand cDNA synthesis kit (Fermentas), and real-time quantitative PCR (qPCR) was subsequently performed in triplicate using SYBR green PCR (Applied Biosystems) on a 7900HT fast real-time PCR system (Applied Biosystems). The following qPCR primer sets were used: GAPDH forward (fw), AGCCACATCGCTCAGACACC; GAPDH reverse (rev), ACCCGTTGACTCCGACCTT; ARIH1 fw, TCATGCCTCTACCCAAGC CTT; and ARIH1 rev, ACCAAACCCACAGCAACACA. Data were collected and analyzed using SDS2.3 software (Applied Biosystems). Relative mRNA levels after correction for glyceraldehyde-3-phosphate dehydrogenase (GAPDH) control mRNA were expressed using the threshold cycle ($2^{-\Delta\Delta CT}$) method.

RESULTS

A ubiquitination RNAi screen identifies CP response modulators. We performed an siRNA-based screen using the Dharmacon ubiquitination SMARTpool library and custom-made SMARTpool libraries targeting all known cellular deubiquitinases (DUBs), sumoylases, and desumoylases (see Table S1 in the supplemental material). Mouse embryonic stem (ES) cells that display a robust apoptotic response to genotoxic compounds, including CP (see Fig. S1A and B in the supplemental material), were treated with 10 μM CP or a vehicle, and cell viability was monitored after 24 h. Fifty SMARTpools were identified that met selection criteria (no significant effect under control conditions; modulation of viability in the presence of CP with a Z-score of ± 1.5 and a P value of >0.05) (Fig. 1A; see also Table S2 in the supplemental material). As controls, we included siRNA SMARTpools either targeting Kif11, expected to induce cell killing already under control conditions due to mitotic spindle defects, or targeting p53, expected to protect ES cells against CP-induced killing. In all experimental plates, siKif11 resulted in ~90% reduction in viability under both control and CP treatment conditions, and sip53 protected against CP-induced loss of viability (see Fig. S1C). As a quality measurement, Z′ factors were calculated based on si-lamin (negative control) and si-p53. The average of calculated Z′ factors was 0.45, indicating a good signal-to-noise ratio and reproducibility of the screens (Fig. S1D). To exclude off-target effects, selected SMARTpools entered a deconvolution screen, where 28/50 hits were confirmed with at least 2/4 sequences reproducing the effect of the SMARTpool (Fig. 1B and C; see also Table S3 in the supplemental material).

The 28 confirmed hits included siRNAs targeting six DUBs, one E1 ubiquitin-activating enzyme, Ube1x, one E2 ubiquitin-conjugating enzyme, UBE2D3, and 12 siRNAs targeting E3 ubiquitin ligases (Fig. 1D). Moreover, we identified seven siRNAs targeting proteins with no described ubiquitinase function that were included in the ThermoFisher "ubiquitination library," presumably based on the presence of predicted domains associated with ubiquitinase function, including RING, SOCS, or SPRY (see Discussion). The knockdown of the E1 ubiquitin enzyme Ube1x (Uba), which has recently been shown to be a crucial E1 enzyme in the DDR following ionizing radiation and replication stress (29), resulted in a particularly strong reduction of viability (Fig. 1C).

Enrichment of p53 modifiers and DNA repair regulators. A large proportion of the identified hits have been previously established to control the levels or activity of the transcription factor

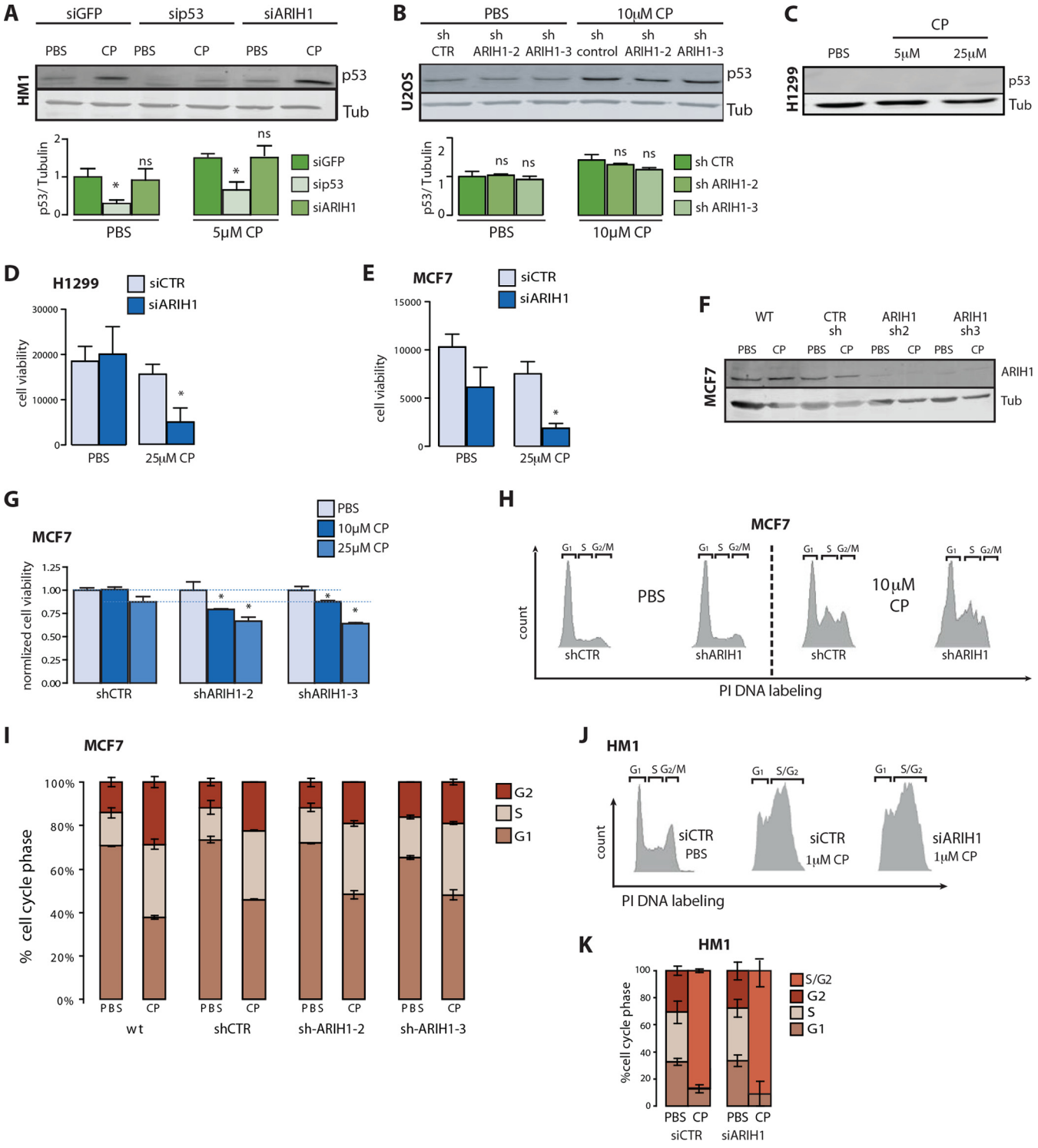

FIG 3 Silencing ARIH1 enhances cell death in response to genotoxic stress in a p53- and caspase-3-independent manner. (A) p53 and tubulin control protein levels in ES cells in the presence of the indicated siRNAs treated with PBS control or 5 μM CP for 8 h. The graph shows quantification of Western blot data ($n = 4$). (B) p53 and tubulin control protein levels in U2OS cells in the presence of control or ARIH1 shRNAs treated with PBS control or 10 μM CP for 16 h. The graph shows quantification of Western blot data ($n = 3$). (C) p53 and tubulin control protein levels in p53-deficient H1299 cells treated with the indicated concentrations of CP for 24 h. Note the absence of p53. (D) H1299 cell viability under control or siARIH1 conditions after treatment with vehicle control PBS or 25 μM CP for 24 h. (E) MCF7 cell viability under control or siARIH1 conditions after treatment with PBS or 25 μM CP for 48 h. (F) ARIH1 and tubulin control protein levels in MCF7 cells bulk puromycin sorted for expression of control shRNA or different shRNAs targeting ARIH1. ARIH1/tubulin ratios normalized to the wild-type (WT) control in the order they appear on the blot were 1.00, 1.78, 1.06, 0.87, 0.04, 0.13, 0.14, and 0.10. (G) Cell viability for sh-control and two shARIH1 MCF7 cell lines treated for 48 h with PBS or 10 or 25 μM CP. (H) Fluorescence-activated cell sorter (FACS) analysis for cell cycle content in sh-control and shARIH1 MCF7 cell lines treated for 24 h with PBS or 10 μM CP. (I) Quantification of cell cycle profiles in wild-type, sh-control, and shARIH1-2 and -3 MCF7 cell lines after treatment with PBS or 10 μM CP for 24 h. (J) FACS profiles for HM1 cell cycle content under control, siGFP, or siARIH1 conditions after treatment with a vehicle control or 1 μM CP. (K) Cell cycle distribution derived from profiles in panel J ($n = 3$). *, $P < 0.05$.

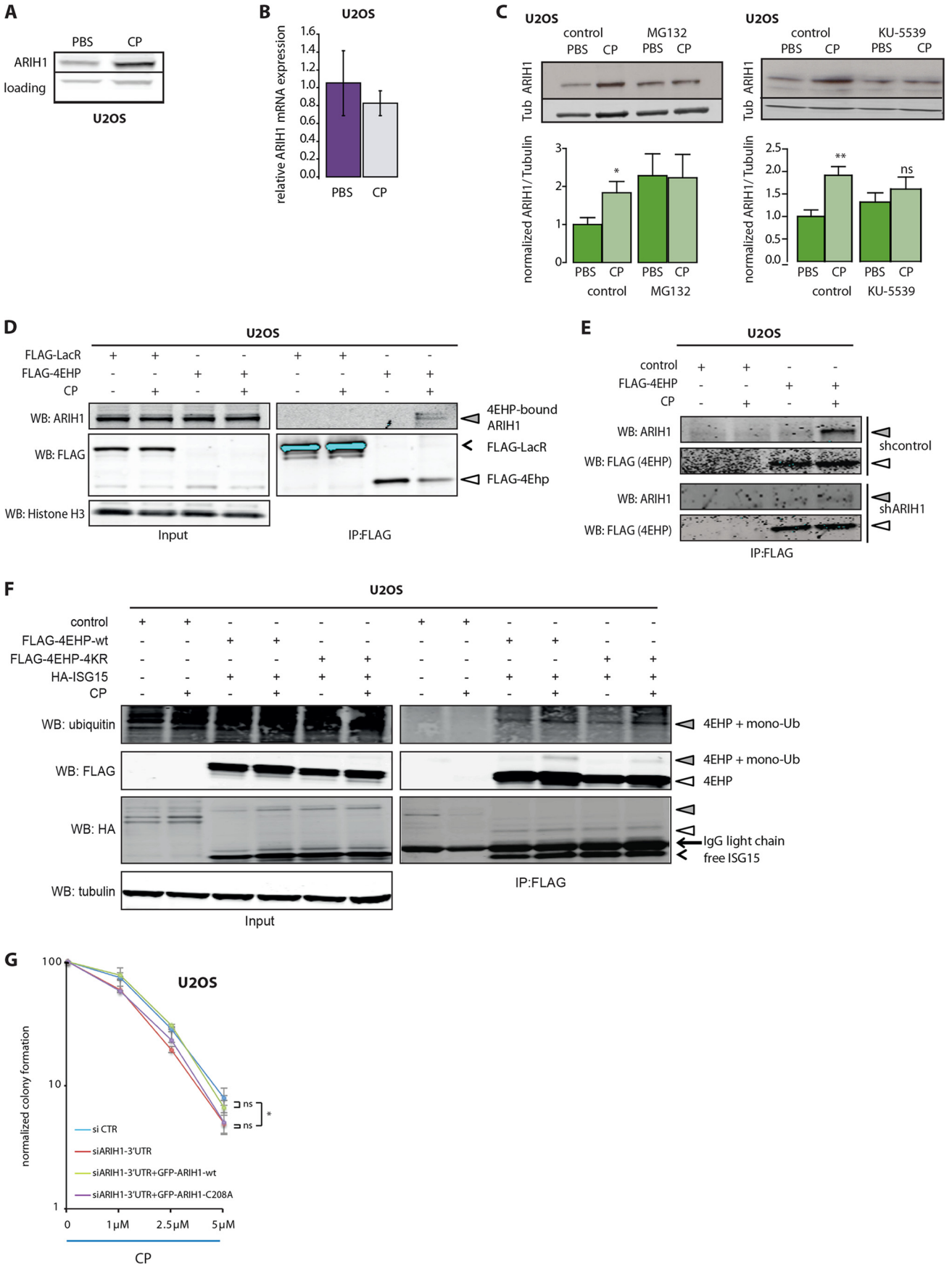
A
PBS
CP
ARIH1
loading
U2OS
B
U2OS
relative ARIH1 mRNA expression
1.6
1.4
1.2
1.0
0.8
0.6
0.4
0.2
0.0
PBS
CP
C
U2OS
control
MG132
PBS CP PBS CP
Tub ARIH1
normalized ARIH1/Tubulin
3
2
1
0
*
PBS CP PBS CP
control MG132
U2OS
control
KU-5539
PBS CP PBS CP
Tub ARIH1
normalized ARIH1/Tubulin
2.5
2.0
1.5
1.0
0.5
0.0
**
ns
PBS CP PBS CP
control KU-5539
D
U2OS
FLAG-LacR + + - - + + - -
FLAG-4EHP - - + + - - + +
CP - + - + - + - +
WB: ARIH1
WB: FLAG
WB: Histone H3
4EHP-bound ARIH1
FLAG-LacR
FLAG-4Ehp
Input
IP:FLAG
E
U2OS
control + + - -
FLAG-4EHP - - + +
CP - + - +
WB: ARIH1
WB: FLAG (4EHP)
shcontrol
WB: ARIH1
WB: FLAG (4EHP)
shARIH1
IP:FLAG
F
U2OS
control + + - - - - + + - - - -
FLAG-4EHP-wt - - + + - - - - + + - -
FLAG-4EHP-4KR - - - - + + - - - - + +
HA-ISG15 - - + + + + - - + + + +
CP - + - + - + - + - + - +
WB: ubiquitin
WB: FLAG
WB: HA
WB: tubulin
4EHP + mono-Ub
4EHP + mono-Ub
4EHP
IgG light chain
free ISG15
Input
IP:FLAG
G
U2OS
normalized colony formation
100
10
1
ns
ns
*
si CTR
siARIH1-3'UTR
siARIH1-3'UTR+GFP-ARIH1-wt
siARIH1-3'UTR+GFP-ARIH1-C208A
0
1 μM
2.5 μM
5 μM
CP

p53, which acts as a master regulator of the outcome of the DDR in various cell types, including ES cells (Fig. 1E) (1, 2, 30). Three of the identified DUBs, USP7 (HAUSP), USP4, and USP5, can directly or indirectly influence p53 protein levels (10, 31–33). In addition, the E3 ligases Rfwd3, Pirh2, and TOPORS were previously shown to affect p53 stability (10, 34, 35) (Fig. 1E; see also Table S3 in the supplemental material). Besides p53 regulators, we identified several other ubiquitin ligases implicated in DDR-related processes, such as postreplication repair (SHPRH [36]), translesion synthesis (Pirh2 [37]), DSB repair (BRCA1 [38]), and the replication protein A (RPA)-mediated repair of single-strand breaks (Rfwd3 [39]), further confirming the validity of the targets identified in our screen.

Silencing of ARIH1 sensitizes to genotoxic stress. One of the strongest hits in the screen was the parkin family ubiquitin ligase ariadne homologue 1 (ARIH1) (40). The ARIH1 SMARTpool and all four of the individual sequences tested in the deconvolution experiments significantly sensitized ES cells to CP-induced loss of viability (Fig. 1A and C; see also Table S3 in the supplemental material). In order to examine if ARIH1 was involved in the response to specific types of stress, the effect of ARIH1 knockdown in ES cells was examined after treatment with various genotoxic and nongenotoxic compounds. All compounds were used at equitoxic doses causing ~50% loss of viability after 24 h of treatment (Fig. 2A). Knockdown of ARIH1, using the SMARTpool or individual siRNAs, did not affect ES cell viability under control conditions (Fig. 2B and C). Similar to its effect on CP sensitivity, silencing of ARIH1 using the SMARTpool or individual siRNAs significantly sensitized ES cells to all tested genotoxic drugs, including the topoisomerase inhibitor etoposide, the DNA intercalator doxorubicin, and the DNA cross-linking compound mitomycin C (Fig. 2B and C). In contrast, knockdown of ARIH1 did not sensitize ES cells to nongenotoxic agents such as the oxidative stressor diethyl maleate (DEM), the ER stressor thapsigargin, or the microtubule poison vincristine (Fig. 2C). Decreased viability as measured in the ATPlite assay correlated with an increased sub-G_0/G_1 fraction in ARIH1-depleted ES cells that could be detected after treatment with a lower dose of CP, pointing to increased cell death (Fig. 2D).

In order to validate these findings in human cancer cells, we examined the effect of silencing ARIH1 in U2OS, p53 wild-type human sarcoma cells. We introduced lentiviral shRNAs targeting ARIH1 and following bulk puromycin selection identified two short hairpins providing ~90% reduction in ARIH1 protein levels (Fig. 2E). Basal cell survival was somewhat reduced compared to that of a lentiviral control cell line (Fig. 2F). Nevertheless, analogous to the effect observed in ES cells, both ARIH1-depleted cell lines showed a significantly increased loss of viability in response to treatment with 10 or 25 μM CP for 48 h (Fig. 2F). Clonogenic survival in a 10-day colony formation assay of ARIH1-depleted U2OS cells was also markedly more impaired by 24 h of pretreatment with a dose range of CP compared to control cells (Fig. 2G). Moreover, silencing of ARIH1 not only led to sensitization to genotoxic compounds but also significantly reduced clonogenic survival after IR (Fig. 2H).

Genotoxic stress-induced ARIH1 accumulation represents a p53- and caspase-3-independent adaptive response. In contrast to reported functions for many of the other identified hits (Fig. 1E; see also Table S3 in the supplemental material), ARIH1 did not control basal or genotoxic stress-induced p53 stability in ES or U2OS cells (Fig. 3A and B). In further disagreement with a role for p53 in the enhanced sensitivity to genotoxic stress observed in ARIH1-depleted cells, silencing of ARIH1 effectively sensitized the p53-deficient non-small-cell lung cancer cell line H1299 (41) to CP (Fig. 3C and D). Transient knockdown of ARIH1 also sensitized the caspase-3-deficient human breast cancer cell line MCF7, indicating that the effect of ARIH1 was not restricted to caspase-3-mediated apoptosis (Fig. 3E). Although less prominent, the same effect was observed using 2 independent MCF7 shARIH1 lines (Fig. 3F and G). DNA damage can trigger a p53-dependent or independent cell cycle arrest (42). In MCF7, ARIH1 knockdown did not alter basal cell cycle distribution or CP-induced increase in S/G_2 (Fig. 3H and I). Likewise, ARIH1 knockdown did not affect basal cell cycle distribution or CP-induced G_2/S arrest in ES cells (Fig. 3J and K). Together, these data indicated that ARIH1-depleted cells display normal arrest of the cell cycle in response to genotoxic stress, while cell survival following DNA damage is compromised in the absence of ARIH1 and this increased sensitivity is independent of p53 or caspase-3-mediated apoptosis.

We tested if DNA damage affected the abundance of ARIH1. ARIH1 protein levels were enhanced following CP treatment in U2OS cells (Fig. 4A). This could not be explained by enhanced mRNA levels, indicating that genotoxic stress triggered increased synthesis or enhanced stability of the ARIH1 protein (Fig. 4B). Treatment with the proteasome inhibitor MG132 led to increased basal ARIH1 levels, with CP treatment not causing further ARIH1 accumulation under these conditions (Fig. 4C). KU-5593, an inhibitor of ATM, a central kinase within the DDR signaling network, blocked CP-induced ARIH1 accumulation, suggesting that DNA damage caused ATM-mediated attenuation of proteasomal

FIG 4 ARIH1 accumulates after DNA damage and interacts with 4EHP. (A) ARIH1 protein levels in U2OS cells treated for 4 h with PBS or 5 μM CP. (B) qPCR analysis of ARIH1 RNA levels, normalized to GAPDH in U2OS cells treated for 4 h with PBS or 5 μM CP. (C) Western blot for ARIH1 and tubulin loading control. For inhibitor treatment, cells were pretreated for 30 min with dimethyl sulfoxide (DMSO) vehicle control, 10 μM proteasome inhibitor MG132, or 5 μM ATM inhibitor KU-55933 and subsequently exposed to 5 μM CP or PBS vehicle control for 4 h in the presence of the indicated inhibitors. Quantification is representative for 4 independent experiments. (D) Total cell lysates and FLAG pulldown of U2OS cells transfected with control FLAG-LacR or FLAG-4EHP plasmids and treated with a vehicle control or 5 μM CP for 4 h, followed by Western blotting (WB) for FLAG or ARIH1. Histone H3 Western blotting on total lysates served as a loading control. (E) FLAG pulldown of U2OS cells bulk puromycin selected for expression of the indicated shRNAs, subsequently transfected with control or FLAG-4EHP cDNAs, and treated with a vehicle control or 5 μM CP for 4 h. Western blots are shown for FLAG (4EHP) and endogenous ARIH1. Open and shaded arrowheads are as defined in panel D. (F) Total cell lysates and FLAG pulldown of U2OS cells transfected with FLAG-tagged wild-type or 4KR mutant 4EHP in combination with HA-ISG15 and treated with a vehicle control or 5 μM CP for 4 h, followed by Western blotting for FLAG, HA, or ubiquitin. Tubulin Western blotting on total lysates served as a loading control. (G) Colony formation capacity after 24 h of treatment with CP at the indicated concentrations in control U2OS cells or U2OS cells stably expressing GFP-tagged wild-type or C208A mutant ARIH1, in the absence or presence of siRNA targeting luciferase (control) or the ARIH1 3′ UTR. Means ± SDs are shown for two independent biological replicates. Data fitting with single exponential decay followed by F-test gave the following *P* values using si CTR as a reference: siARIH1-3′ UTR, $P = 0.0195$; siARIH1-3′ UTR plus GFP-ARIH1-WT, $P = 0.7548$; and siARIH1-3′ UTR plus GFP-ARIH1-C208A, $P = 0.0201$. *, $P < 0.05$. ns, not significant.

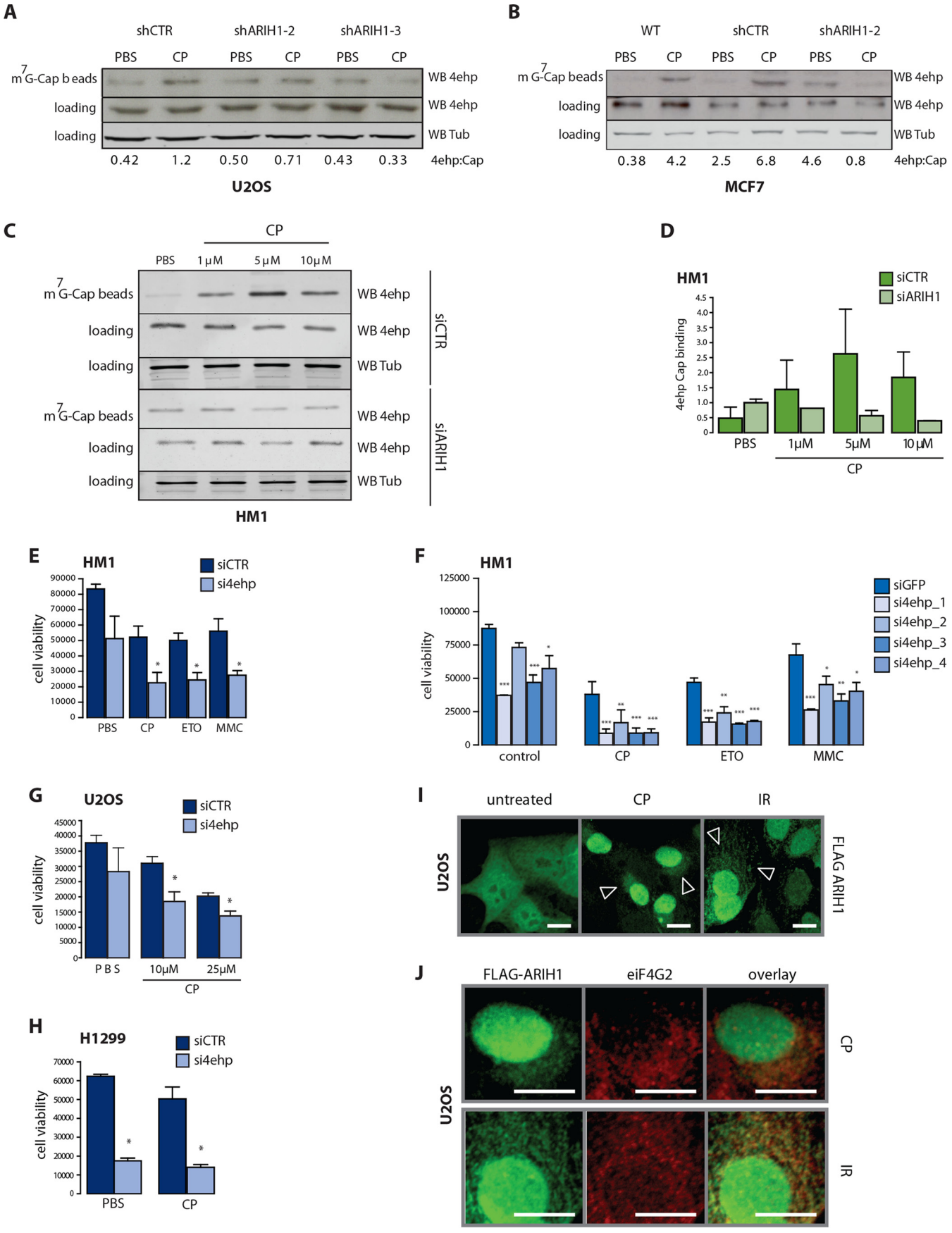
A
shCTR
shARIH1-2
shARIH1-3
PBS
CP
m7G-Cap beads
loading
loading
WB 4ehp
WB 4ehp
WB Tub
0.42 1.2 0.50 0.71 0.43 0.33
4ehp:Cap
U2OS
B
WT
shCTR
shARIH1-2
0.38 4.2 2.5 6.8 4.6 0.8
MCF7
C
CP
PBS
1 µM
5 µM
10µM
siCTR
siARIH1
HM1
D
HM1
siCTR
siARIH1
4ehp Cap binding
PBS
1µM
5µM
10 µM
CP
E
HM1
siCTR
si4ehp
cell viability
PBS
CP
ETO
MMC
F
HM1
siGFP
si4ehp_1
si4ehp_2
si4ehp_3
si4ehp_4
cell viability
control
CP
ETO
MMC
G
U2OS
siCTR
si4ehp
cell viability
PBS
10µM
25µM
CP
H
H1299
siCTR
si4ehp
cell viability
PBS
CP
I
untreated
CP
IR
U2OS
FLAG ARIH1
J
FLAG-ARIH1
eiF4G2
overlay
U2OS
CP
IR

degradation of ARIH1 (Fig. 4C). We tested whether regulation of ARIH1 abundance might occur through suppression of self-ubiquitination. However, although ARIH1 appeared to be ubiquitinated, this modification was not regulated by CP and was unaffected by ATM inhibition (see Fig. S2A in the supplemental material). Moreover, a ubiquitination-deficient ARIH1 mutant (C208A mutant) displayed a markedly similar ubiquitination pattern (24). Notably, MS analysis of GFP-ARIH1 immunoprecipitations identified K144 as a ubiquitinated site in ARIH1, yet again, this was not modulated by CP treatment (see Fig. S2B). We also identified multiple ARIH1-interacting components of the ubiquitination machinery (i.e., ubiquitin itself, the E1 enzyme UBA1, and the E2 enzyme UBE2L3, known to interact with ARIH1). Such interactions, as well as a potential product (K48 polyubiquitin chains), were moderately increased upon CP treatment (see Fig. S2B).

CP treatment induces 4EHP ubiquitination. In response to DNA damage, ongoing cellular activities are suppressed, while stress programs and DNA repair processes are activated. One typical response is the acute inhibition of protein synthesis through alterations of the cap-dependent translation initiation complex (43). This can be achieved in several ways, including recruitment of 4EHP (eIF4E2), a competitive inhibitor of the canonical cap-binding translation initiation factor, eIF4E (20). In contrast to eIF4E, 4EHP cannot bind the structural component eIF4G that is required for ribosome recruitment and subsequent mRNA translation. Although ARIH1 can act as an E3 ubiquitin ligase for 4EHP (44), there is also evidence that ARIH1 can ISGylate 4EHP, thus enhancing its affinity for the mRNA cap structure and its ability to replace eIF4E (23). Coimmunoprecipitations with U2OS cells showed that the increased abundance of ARIH1 in CP-treated cells was accompanied by increased association of ARIH1 with 4EHP and that this 4EHP-associated ARIH1 was lost in shARIH1 cells (Fig. 4D and E).

Next, we analyzed CP-induced posttranslational modification of wild-type 4EHP and a K121/130/134/222R (4KR) mutant that cannot be ISGylated (23). Immunoprecipitation of wild-type 4EHP showed bands of higher molecular weight appearing upon CP treatment (Fig. 4F). Identical bands were also observed for the 4KR-4EHP mutant, arguing against 4EHP-ISGylation. Moreover, such species were detected by a ubiquitin antibody, whereas Western blotting for coexpressed HA-ISG15 did not detect these species, despite the fact that free ISG15 was readily detected in the FLAG immunoprecipitations. The most prominent modification observed corresponded to 4EHP modified with one ubiquitin molecule (28 + 7 kDa) and to a lesser extent diubiquitination, but not polyubiquitination, associated with a degradative mark (6).

ARIH1 ubiquitination function mediates adaptation to genotoxic stress. Results thus far suggested that 4EHP is ubiquitinated, rather than ISGylated, after genotoxic stress. We tested whether the ISGylation or ubiquitination function of ARIH1 was required for its protective role in genotoxic stress. Therefore, we silenced ARIH1 using an siRNA targeting the 3′ UTR in U2OS cells expressing either wild-type ARIH1 or a C208A mutant that fails to associate with the E2 enzyme UbcH7, rendering it defective in ubiquitination (whereas interaction with UbcH8 and hence ISGylase activity are intact) (24). Again, ARIH1-silenced cells were more sensitive to CP treatment, although the effect of the transient siRNA was less prominent than stable shRNA-mediated silencing (see Fig. 2G). Expression of wild-type but not ubiquitination-deficient (C208A) ARIH1 restored colony formation capacity under genotoxic stress in siARIH1 cells (Fig. 4G).

Together, these data indicate that 4EHP ubiquitination constitutes the predominant modification induced by genotoxic stress and that ARIH1 ubiquitinase function is crucial for its protective role in the genotoxic stress response.

CP treatment induces 4EHP cap binding and translation arrest in an ARIH1-dependent manner. ARIH1-dependent ISGylation has been reported to regulate 4EHP association with the mRNA 5′ cap, but ARIH1-mediated ubiquitination of 4EHP, although described, is not known to affect this process. In order to clarify whether ARIH1 supported 4EHP translocation to the mRNA cap upon CP treatment, we used 5′ 7-methylguanosine cap pulldown assays. Indeed, 4EHP binding to the mRNA cap was induced in response to CP in U2OS, MCF7, and ES cells (Fig. 5A to D). Importantly, this response was dependent on ARIH1, as CP-induced 4EHP-cap association was abrogated in U2OS, MCF7, and ES cells upon ARIH1 depletion (Fig. 5A to D). Subsequently, to test if 4EHP-cap association represents an ARIH1-regulated pathway that is involved in protection against CP, 4EHP itself was silenced. In line with such a function, ES cells and U2OS cells were sensitized to genotoxic compounds following 4EHP silencing, and viability of H1299 in the presence of CP and control conditions was compromised (Fig. 5E to H).

These findings indicated that the ability of ARIH1 to protect against genotoxic stress-induced cell death involves 4EHP-mediated translation inhibition at the mRNA 5′ cap. To address whether ARIH1 localized at sites of mRNA translation upon genotoxic stress, we performed immunostainings to assess subcellular localization of ARIH1. Whereas in untreated U2OS cells ARIH1 resided in the nucleus and diffusely throughout the cytoplasm, treatment with CP or IR caused ARIH1 concentration at both the nucleus and speckled structures in perinuclear regions, which markedly resemble ribosomes (Fig. 5H). In agreement with a genotoxic stress-induced transition of ARIH1 to ribosomes, and a role in 4EHP-mediated translation arrest, eIF4G2, a ribosomal marker, colocalized to such ARIH1-containing perinuclear regions upon either CP treatment or IR (Fig. 5I and J).

FIG 5 ARIH1 mediates DNA damage-induced cap binding of 4EHP. (A to C) m^7G cap pulldown from control and ARIH1-silenced U2OS (A), MCF7 (B), and HM1 ES (C) cells treated with a vehicle control or the indicated concentrations of CP, followed by Western blotting for 4EHP or tubulin control. Numbers at the bottoms of panels A and B indicate cap-associated 4EHP levels relative to total 4EHP. (D) Quantification of m^7G cap-bound 4EHP in control siGFP and siARIH1 ES cells (2 independent experiments). (E) ES cell viability under si-control or si4EHP conditions after treatment with PBS, 10 μM CP, 150 nM etoposide (ETO), or 10 μg/μl of mitomycin C (MMC) for 24 h. (F) ES cell viability in the presence of siRNAs targeting GFP or 4 individual sequences targeting 4EHP after control treatment or treatment with 10 μM CP, 150 nM ETO, or 10 μg/μl of MMC. (G) U2OS cell viability under si-control (siGAPDH) or si4EHP conditions after treatment with PBS or 10 or 25 μM CP. (H) H1299 cell viability under si-control or si4EHP conditions after treatment with PBS or 25 μM CP. (I) FLAG-ARIH1 localization before or after treatment with 5 μM CP for 4 h or 4 h after treatment with 2 Gy of IR. Arrowheads indicate regions of perinuclear accumulation. (J) Higher magnification of perinuclear staining for FLAG-ARIH1 (green), ribosomal marker eIF4G2 (red) staining, and overlay after CP treatment or IR. Bars (I and J), 5 μm. *, $P < 0.05$; **, $P < 0.01$.

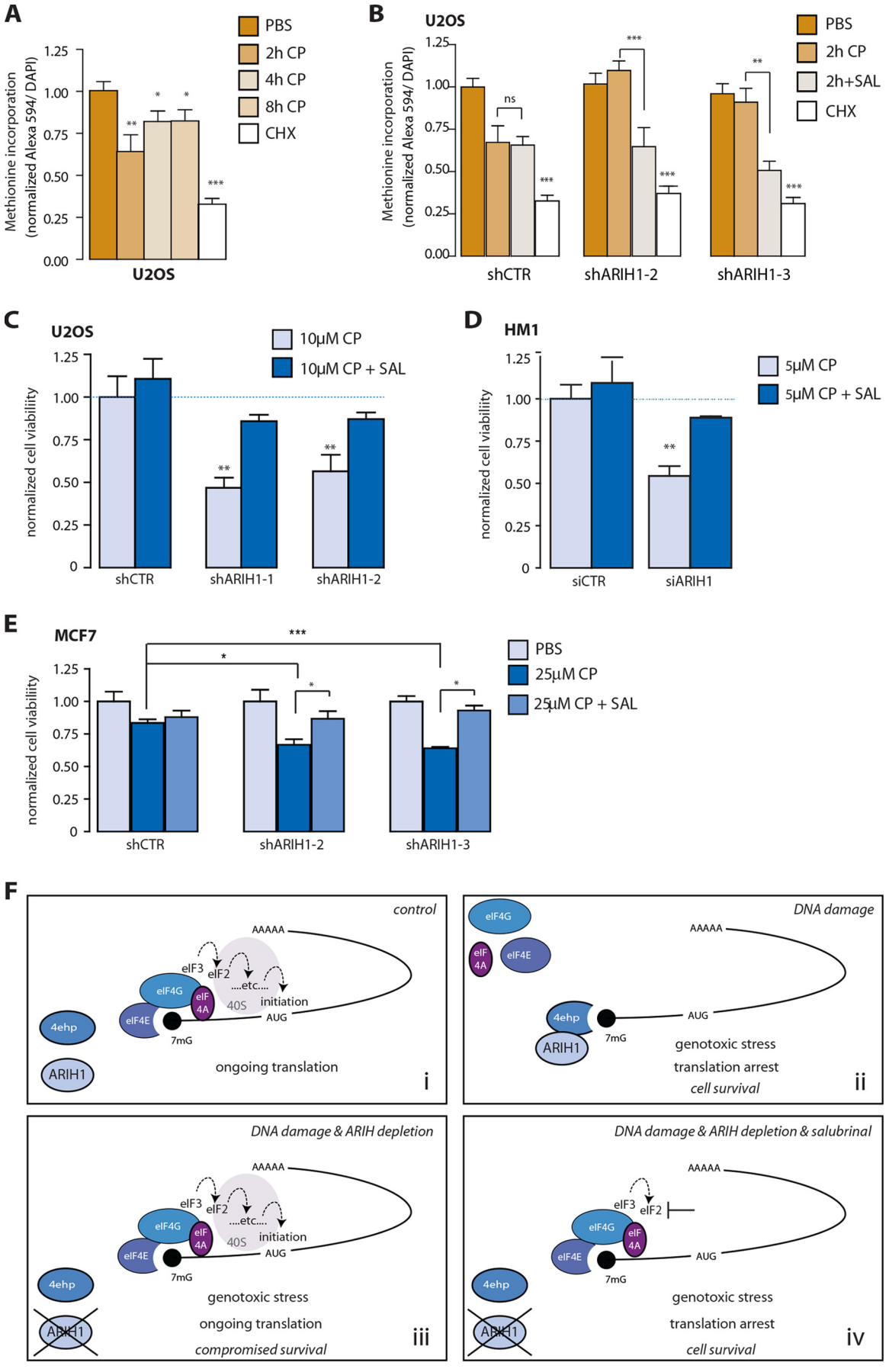
A
PBS
2h CP
4h CP
8h CP
CHX
Methionine incorporation (normalized Alexa 594/ DAPI)
U2OS
B
U2OS
PBS
2h CP
2h+SAL
CHX
Methionine incorporation (normalized Alexa 594/ DAPI)
ns
shCTR
shARIH1-2
shARIH1-3
C
U2OS
10μM CP
10μM CP + SAL
normalized cell viability
shCTR
shARIH1-1
shARIH1-2
D
HM1
5μM CP
5μM CP + SAL
normalized cell viability
siCTR
siARIH1
E
MCF7
PBS
25μM CP
25μM CP + SAL
normalized cell viability
shCTR
shARIH1-2
shARIH1-3
F
control
AAAAA
eIF3
eIF2
....etc....
initiation
eIF4G
eIF 4A
40S
eIF4E
AUG
7mG
4ehp
ARIH1
ongoing translation
i
DNA damage
genotoxic stress
translation arrest
cell survival
ii
DNA damage & ARIH depletion
genotoxic stress
ongoing translation
compromised survival
iii
DNA damage & ARIH depletion & salubrinal
genotoxic stress
translation arrest
cell survival
iv

To directly address whether ARIH1 was important for inducing a DNA damage-induced translation arrest, Click-iT metabolic labeling was used to quantify newly synthesized proteins. CP treatment caused a significant translation arrest in U2OS cells, with a 30% reduction of protein synthesis at 2 h posttreatment and maintenance of a 25% reduction at 4 and 8 h posttreatment (Fig. 6A). In line with a critical role for ARIH1 in mediating this arrest, two independent shARIH1 lines did not show this CP-induced translation arrest. Notably, a 60% reduction in translation caused by cycloheximide in wild-type U2OS remained intact in ARIH1-silenced cells (Fig. 6A and B).

Finally, we investigated if the ARIH1-mediated translation arrest was critical for the role of ARIH1 in adaptation to genotoxic stress. For this, we made use of salubrinal, an inhibitor of eIF2α dephosphorylation that renders the eIF2 initiation factor inactive and inhibits mRNA translation under stress conditions. Cotreatment with salubrinal restored the CP-induced translation arrest in ARIH1-depleted cells (Fig. 6B). Indeed, such an alternatively triggered translation arrest significantly restored viability of CP-treated ARIH1-silenced U2OS, ES, and MCF7 cells (Fig. 6C to E).

Together, these findings indicate that DNA damage induces an increase in ARIH1 protein levels and association of ARIH1 with 4EHP. In turn, this causes 4EHP recruitment to the mRNA cap, where it is known to compete with eIF4E. The resulting mRNA translation arrest represents an adaptive response to genotoxic stress: ARIH1 depletion sensitizes cells to genotoxic stress, while reestablishing the translation arrest at the level of eIF2 with salubrinal alleviates this effect (Fig. 6F).

DISCUSSION

Ubiquitination plays a vital role in the DDR signal transduction cascade. Our RNAi screen targeting the cellular ubiquitination and sumoylation machinery identifies several genes that modulate the response to the chemotherapeutic drug CP. Some of the identified DUBs and E3 ubiquitin ligases have previously been implicated in p53 regulation or DNA repair processes (5, 10). In addition, the screen identifies genes associated with cell cycle control or developmental processes. These include Fbxw7, a tumor suppressor that marks several proto-oncogenes, such as the Myc, Jun, cyclin E, and Notch genes, for degradation, and Dtx2, an E3 ligase also proposed to control the Notch signaling pathway (45–47). Which of these functions explains the role of these ubiquitin ligases in the response to genotoxic stress is not known. Moreover, while two of the individual siRNAs mimicked the SMARTpool for these genes, the deconvolution screen also revealed one individual siRNA for these genes to have the opposite effect. This indicates that either of those outcomes is likely an off-target effect, and further experiments are required to determine the role of these genes in the response to genotoxic stress. We also identified another F box protein, Fbx017, with which the SMARTpool and 3/4 individual siRNAs caused sensitization, providing more firm confidence in a potential role for this gene in adaptation to genotoxic stress. However, no mechanism of action has been described for Fbx017 yet.

Another group of identified hits has been associated with intracellular transport processes, including the DUB USP8, which regulates endosomal sorting of membrane receptors, and RUFY and SYTL4, which are involved in Rab-mediated vesicular transport (48–50).

Notably, some of the hits from the "ubiquitination SMARTpool library" do not have an established (de)ubiquitinase function. These include (i) the zinc finger-containing chromatin remodeling factor CHD4, which lacks domains associated with (de)ubiquitinase activity (51); (ii) the Rab-interacting proteins RUFY and SYTL4, which have an FYVE zinc finger domain which is structurally similar to the RING domain (49, 50); and (iii) TCE1 and Rspry1, containing a SPRY domain that is found in members of the TRIM family of ubiquitin ligases (52). In addition, Rspry1 contains a RING domain and TCE1 also harbors a SOCS box domain, which mediates interactions with the elongin BC complex, an adaptor module in E3 ubiquitin ligase complexes (53).

The parkin family ubiquitin ligase ARIH1 has not been previously implicated in DDR signaling. Our findings reveal that ARIH1 protects pluripotent stem cells as well as various cancer cells from the toxic effects of genotoxic chemical agents and IR that cause DSBs. The cytoprotective role of ARIH1 is also observed in cancer cells lacking a functional p53 or caspase-3 response. Hence, ARIH1 is not required specifically for dampening p53-induced, caspase-3-mediated apoptosis. Instead, we find that ARIH1 mediates an mRNA translation arrest in response to DNA damage by binding to 4EHP and stimulating its recruitment to the mRNA 5′ cap.

The obstruction of mRNA translation is an important event in the response to cellular stress, and alterations in this regulatory hub have been suggested to be important for resistance of cancer cells to therapy (19, 54). A well-described mechanism for translation repression is enhanced interaction of the cap-binding protein eIF4E with its negative regulator eIF4-BP1. Under normal conditions, this interaction is suppressed by mTOR-mediated phosphorylation of eIF4-BP1 (55). Alternative eIF4E-dependent and independent mechanisms for translation repression have been described (20). For instance, impaired Met tRNA recruitment, through eIF2α Ser51 phosphorylation, represents a canonical response to accumulation of improperly folded proteins in the endoplasmic reticulum: the so-called unfolded protein response

FIG 6 ARIH1 mediates CP-induced mRNA translation arrest. (A) Methionine incorporation in U2OS cells after treatment with 15 μM CP for 2 h, 4 h, or 8 h or with 2 mg/ml of cycloheximide (CHX) for 1 h. Alexa Fluor 546 signal (reflecting amount of newly synthesized protein)/number of nuclei (DAPI), normalized to the PBS condition, is shown. (B) Methionine incorporation in sh-control and two different shARIH1 U2OS cell lines after treatment with 2 mg/ml of CHX for 1 h, 15 μM CP for 2 h, or cotreatment with 15 μM CP and 2.5 μM salubrinal (SAL) for 2 h. Alexa Fluor 546 signal/number of nuclei, normalized to the PBS condition, is shown. (C to E) Cell survival in cells expressing indicated siRNAs or shRNAs after treatment with the indicated concentrations of CP in the absence or presence of 2.5 μM SAL. (C) U2OS cells with 48 h of treatment; (D) ES cells with 24 h of treatment; (E) MCF7 cells with 48 h of treatment. (F) Model for the role of ARIH1 in regulating sensitivity to genotoxic stress. (i) Under nonstress conditions, eIF4E binds the mRNA 5′ 7-methylguanosine cap, a preinitiation complex is formed that scans the mRNA until the AUG codon is found, and translation can occur. (ii) Upon genotoxic stress, ARIH1 accumulates and associates with 4EHP, resulting in recruitment of 4EHP to the 5′ cap, where it replaces eIF4E, thereby disrupting the preinitiation complex and resulting in translation arrest that is cytoprotective. (iii) In the absence of ARIH1, 4EHP is not recruited to the mRNA 5′ cap, DNA damage-induced translation arrest does not occur, and cell survival is compromised. (iv) Restoration of the translation arrest in ARIH1-depleted cells experiencing genotoxic stress by preventing formation of a preinitiation complex through inhibition of eIF2 also restores cell survival.

(56). Yet another way to arrest mRNA translation is through enhanced mRNA 5′ cap binding of eIF4E2, also known as 4EHP (57). Our findings implicate the latter mechanism in the DNA damage-induced protein synthesis arrest and provide evidence that it is regulated through ARIH1.

4EHP is an eIF4E homologue that has low affinity for binding the cap structures of most mRNAs (58). The protein has been implicated in the regulation of translation of a specific subset of mRNAs in *Drosophila* involved in embryonic patterning (59, 60). ARIH1 can ISGylate 4EHP, resulting in increased mRNA 5′ cap affinity, but it is not known under which conditions ARIH1-mediated ISGylation of 4EHP is induced (23). Here, we demonstrate that in response to DSB-inducing genotoxic stress, ARIH1 protein accumulates and interacts with 4EHP, leading to increased recruitment of 4EHP to the mRNA 5′ cap. Our findings obtained using a non-ISGylatable 4EHP mutant and 4EHP:ISG15 coimmunoprecipitations indicate that ubiquitination but not ISGylation is the predominant DNA damage-induced 4EHP modification. Moreover, we show that ubiquitination capacity is required for the ARIH1-mediated adaptive response to genotoxic stress.

The accumulation of ARIH1 depends on activity of ATM, a key kinase in the DDR, and most likely involves inhibition of proteosomal degradation. Despite a putative ATM target motif (S-Q) in the ARIH1 protein at serine 514, phosphorylation of this site has not been detected by us or by other groups in the presence or absence of genotoxic stress (3, 61, 62; unpublished data) (http://www.phosphosite.org). Although this may also be an outcome of technical limitations of the MS used in these studies (for example, a very short tryptic fragment), it points to an indirect mechanism by which ATM signaling leads to ARIH1 accumulation after genotoxic stress. One possible mechanism would involve attenuation of ARIH1 self-ubiquitination following genotoxic stress. However, our results thus far do not suggest autoubiquitination, or its regulation by genotoxic stress or ATM, as the relevant mechanism. It is revealing that our MS analysis indicates that ARIH1 is part of a complex of ubiquitination-related enzymes that is sensitive to genotoxic stress. The detailed composition of this complex and its regulation in response to genotoxic stress will be the topic of further study.

Translation arrest is effectuated by 4EHP due to its capacity to act as a competitive inhibitor for eIF4E. Unlike eIF4E, 4EHP cannot bind the structural component eIF4G required for formation of the preinitiation complex. In line with this, 4EHP was unable to complement eIF4E in gene knockout experiments with *Saccharomyces cerevisiae* (63). Our findings indicate that ARIH1-mediated 4EHP recruitment to the mRNA 5′ cap underlies the cytoprotective role of ARIH1: (i) DNA damage-induced recruitment of 4EHP to the mRNA 5′ cap is ARIH1 dependent, (ii) DNA damage-induced translation arrest is ARIH1 dependent, and (iii) RNAi targeting ARIH1 or 4EHP sensitizes ES or cancer cells to DNA damage. In H1299 cells, 4EHP depletion also compromises viability under control conditions, which may be related to endogenous genotoxic stress. Our data do not support the idea that a genotoxic stress-induced mRNA translation arrest is lost in cancer cells as was described for other eIF4E-dependent routes, such as 4EBP-1 phosphorylation (19). U2OS cells do attenuate protein synthesis following genotoxic stress, and depletion of ARIH1 leads to sensitization of all cancer cell lines tested thus far. Intriguingly, while inhibition of eIF4E cap binding can sensitize cancer cells to different chemotherapeutics (19, 54), we show that inhibition of the competitive process involving ARIH1 and 4EHP has the same effect. Clearly, ongoing mRNA 5′ cap-mediated translation as well as the ability to temporarily arrest translation in response to DNA damage is required for (cancer) cells to escape genotoxic stress-induced death. Our immunofluorescence experiments indicate that upon genotoxic stress, ARIH1 is concentrated not only in nuclei but also in a perinuclear region where ribosomes are clustered, placing ARIH1 at the correct location to control this process.

As mentioned above, an alternative route to attenuate protein synthesis is through eIF2α Ser51 phosphorylation, a modification typically triggered by an accumulation of misfolded proteins in the ER (56). This response can be enhanced by salubrinal, an inhibitor of the phosphatase complex that dephosphorylates eIF2α (64). Interestingly, treatment with salubrinal restores the CP-induced translation arrest as well as cell survival in ARIH1-depleted cells. This shows that alternative means for attenuating protein synthesis can compensate for the inability to do so through enhanced 4EHP-cap binding. Moreover, it provides further evidence for a model in which the ability of ARIH1 to couple DSB-induced genotoxic stress to attenuation of mRNA translation underlies its cytoprotective role.

ACKNOWLEDGMENTS

We are grateful to Rob Hoeben, Dong-Er Zhang, Martijn Rabelink, and Klaus Willecke for generously providing cells and reagents.

This work was supported by the Netherlands Genomics Initiative/Netherlands Organization for Scientific Research (NWO), grant no. 050-060-510.

We declare that we have no conflict of interest.

REFERENCES

1. **Ciccia A, Elledge SJ.** 2010. The DNA damage response: making it safe to play with knives. Mol Cell **40:**179–204. http://dx.doi.org/10.1016/j.molcel.2010.09.019.
2. **Jackson SP, Bartek J.** 2009. The DNA-damage response in human biology and disease. Nature **461:**1071–1078. http://dx.doi.org/10.1038/nature08467.
3. **Matsuoka S, Ballif BA, Smogorzewska A, McDonald ER 3rd, Hurov KE, Luo J, Bakalarski CE, Zhao Z, Solimini N, Lerenthal Y, Shiloh Y, Gygi SP, Elledge SJ.** 2007. ATM and ATR substrate analysis reveals extensive protein networks responsive to DNA damage. Science **316:**1160–1166. http://dx.doi.org/10.1126/science.1140321.
4. **Reinhardt HC, Yaffe MB.** 2009. Kinases that control the cell cycle in response to DNA damage: Chk1, Chk2, and MK2. Curr Opin Cell Biol **21:**245–255. http://dx.doi.org/10.1016/j.ceb.2009.01.018.
5. **Bergink S, Jentsch S.** 2009. Principles of ubiquitin and SUMO modifications in DNA repair. Nature **458:**461–467. http://dx.doi.org/10.1038/nature07963.
6. **Komander D.** 2009. The emerging complexity of protein ubiquitination. Biochem Soc Trans **37:**937–953. http://dx.doi.org/10.1042/BST0370937.
7. **Morris JR.** 2010. More modifiers move on DNA damage. Cancer Res **70:**3861–3863. http://dx.doi.org/10.1158/0008-5472.CAN-10-0468.
8. **Skaug B, Chen ZJ.** 2010. Emerging role of ISG15 in antiviral immunity. Cell **143:**187–190. http://dx.doi.org/10.1016/j.cell.2010.09.033.
9. **Staub O.** 2004. Ubiquitylation and isgylation: overlapping enzymatic cascades do the job. Sci STKE **2004:**pe43. http://dx.doi.org/10.1126/stke.2452004pe43.
10. **Brooks CL, Gu W.** 2006. p53 ubiquitination: Mdm2 and beyond. Mol Cell **21:**307–315. http://dx.doi.org/10.1016/j.molcel.2006.01.020.
11. **Crosetto N, Bienko M, Dikic I.** 2006. Ubiquitin hubs in oncogenic networks. Mol Cancer Res **4:**899–904. http://dx.doi.org/10.1158/1541-7786.MCR-06-0328.
12. **Wood LM, Sankar S, Reed RE, Haas AL, Liu LF, McKinnon P, Desai SD.** 2011. A novel role for ATM in regulating proteasome-mediated protein degradation through suppression of the ISG15 conjugation pathway. PLoS One **6:**e16422. http://dx.doi.org/10.1371/journal.pone.0016422.

13. **Kerscher O, Felberbaum R, Hochstrasser M.** 2006. Modification of proteins by ubiquitin and ubiquitin-like proteins. Annu Rev Cell Dev Biol **22:**159–180. http://dx.doi.org/10.1146/annurev.cellbio.22.010605.093503.
14. **Nagy V, Dikic I.** 2010. Ubiquitin ligase complexes: from substrate selectivity to conjugational specificity. Biol Chem **391:**163–169. http://dx.doi.org/10.1515/BC.2010.021.
15. **Wenzel DM, Lissounov A, Brzovic PS, Klevit RE.** 2011. UBCH7 reactivity profile reveals parkin and HHARI to be RING/HECT hybrids. Nature **474:**105–108. http://dx.doi.org/10.1038/nature09966.
16. **Reinhardt HC, Cannell IG, Morandell S, Yaffe MB.** 2011. Is post-transcriptional stabilization, splicing and translation of selective mRNAs a key to the DNA damage response? Cell Cycle **10:**23–27. http://dx.doi.org/10.4161/cc.10.1.14351.
17. **Braunstein S, Badura ML, Xi Q, Formenti SC, Schneider RJ.** 2009. Regulation of protein synthesis by ionizing radiation. Mol Cell Biol **29:**5645–5656. http://dx.doi.org/10.1128/MCB.00711-09.
18. **Connolly E, Braunstein S, Formenti S, Schneider RJ.** 2006. Hypoxia inhibits protein synthesis through a 4E-BP1 and elongation factor 2 kinase pathway controlled by mTOR and uncoupled in breast cancer cells. Mol Cell Biol **26:**3955–3965. http://dx.doi.org/10.1128/MCB.26.10.3955-3965.2006.
19. **Silvera D, Formenti SC, Schneider RJ.** 2010. Translational control in cancer. Nat Rev Cancer **10:**254–266. http://dx.doi.org/10.1038/nrc2824.
20. **Kong J, Lasko P.** 2012. Translational control in cellular and developmental processes. Nat Rev Genet **13:**383–394. http://dx.doi.org/10.1038/nrg3184.
21. **Gross JD, Moerke NJ, von der Haar T, Lugovskoy AA, Sachs AB, McCarthy JE, Wagner G.** 2003. Ribosome loading onto the mRNA cap is driven by conformational coupling between eIF4G and eIF4E. Cell **115:**739–750. http://dx.doi.org/10.1016/S0092-8674(03)00975-9.
22. **Gingras AC, Raught B, Sonenberg N.** 1999. eIF4 initiation factors: effectors of mRNA recruitment to ribosomes and regulators of translation. Annu Rev Biochem **68:**913–963. http://dx.doi.org/10.1146/annurev.biochem.68.1.913.
23. **Okumura F, Zou W, Zhang DE.** 2007. ISG15 modification of the eIF4E cognate 4EHP enhances cap structure-binding activity of 4EHP. Genes Dev **21:**255–260. http://dx.doi.org/10.1101/gad.1521607.
24. **Ardley HC, Tan NG, Rose SA, Markham AF, Robinson PA.** 2001. Features of the parkin/ariadne-like ubiquitin ligase, HHARI, that regulate its interaction with the ubiquitin-conjugating enzyme, Ubch7. J Biol Chem **276:**19640–19647. http://dx.doi.org/10.1074/jbc.M011028200.
25. **Campeau E, Ruhl VE, Rodier F, Smith CL, Rahmberg BL, Fuss JO, Campisi J, Yaswen P, Cooper PK, Kaufman PD.** 2009. A versatile viral system for expression and depletion of proteins in mammalian cells. PLoS One **4:**e6529. http://dx.doi.org/10.1371/journal.pone.0006529.
26. **Birmingham A, Selfors LM, Forster T, Wrobel D, Kennedy CJ, Shanks E, Santoyo-Lopez J, Dunican DJ, Long A, Kelleher D, Smith Q, Beijersbergen RL, Ghazal P, Shamu CE.** 2009. Statistical methods for analysis of high-throughput RNA interference screens. Nat Methods **6:**569–575. http://dx.doi.org/10.1038/nmeth.1351.
27. **Puigvert JC, de Bont H, van de Water B, Danen EH.** 2010. High-throughput live cell imaging of apoptosis. Curr Protoc Cell Biol Chapter 18:Unit 18.10. http://dx.doi.org/10.1002/0471143030.cb1810s47.
28. **Moody CA, Scott RS, Amirghahari N, Nathan CO, Young LS, Dawson CW, Sixbey JW.** 2005. Modulation of the cell growth regulator mTOR by Epstein-Barr virus-encoded LMP2A. J Virol **79:**5499–5506. http://dx.doi.org/10.1128/JVI.79.9.5499-5506.2005.
29. **Moudry P, Lukas C, Macurek L, Hanzlikova H, Hodny Z, Lukas J, Bartek J.** 2012. Ubiquitin-activating enzyme UBA1 is required for cellular response to DNA damage. Cell Cycle **11:**1573–1582. http://dx.doi.org/10.4161/cc.19978.
30. **Puigvert JC, von Stechow L, Siddappa R, Pines A, Bahjat M, Haazen LCJM, Olsen JV, Vrieling H, Meerman JHN, Mullenders LHF, van de Water B, Danen EHJ.** 2013. Systems biology approach identifies the kinase Csnk1a1 as a regulator of the DNA damage response in embryonic stem cells. Sci Signal **6:**ra5. http://dx.doi.org/10.1126/scisignal.2003208.
31. **Dayal S, Sparks A, Jacob J, Allende-Vega N, Lane DP, Saville MK.** 2009. Suppression of the deubiquitinating enzyme USP5 causes the accumulation of unanchored polyubiquitin and the activation of p53. J Biol Chem **284:**5030–5041. http://dx.doi.org/10.1074/jbc.M805871200.
32. **Meulmeester E, Maurice MM, Boutell C, Teunisse AF, Ovaa H, Abraham TE, Dirks RW, Jochemsen AG.** 2005. Loss of HAUSP-mediated deubiquitination contributes to DNA damage-induced destabilization of Hdmx and Hdm2. Mol Cell **18:**565–576. http://dx.doi.org/10.1016/j.molcel.2005.04.024.
33. **Zhang X, Berger FG, Yang J, Lu X.** 2011. USP4 inhibits p53 through deubiquitinating and stabilizing ARF-BP1. EMBO J **30:**2177–2189. http://dx.doi.org/10.1038/emboj.2011.125.
34. **Fu X, Yucer N, Liu S, Li M, Yi P, Mu JJ, Yang T, Chu J, Jung SY, O'Malley BW, Gu W, Qin J, Wang Y.** 2010. RFWD3-Mdm2 ubiquitin ligase complex positively regulates p53 stability in response to DNA damage. Proc Natl Acad Sci U S A **107:**4579–4584. http://dx.doi.org/10.1073/pnas.0912094107.
35. **Yang X, Li H, Zhou Z, Wang WH, Deng A, Andrisani O, Liu X.** 2009. Plk1-mediated phosphorylation of Topors regulates p53 stability. J Biol Chem **284:**18588–18592. http://dx.doi.org/10.1074/jbc.C109.001560.
36. **Lin JR, Zeman MK, Chen JY, Yee MC, Cimprich KA.** 2011. SHPRH and HLTF act in a damage-specific manner to coordinate different forms of postreplication repair and prevent mutagenesis. Mol Cell **42:**237–249. http://dx.doi.org/10.1016/j.molcel.2011.02.026.
37. **Jung YS, Hakem A, Hakem R, Chen X.** 2011. Pirh2 E3 ubiquitin ligase monoubiquitinates DNA polymerase eta to suppress translesion DNA synthesis. Mol Cell Biol **31:**3997–4006. http://dx.doi.org/10.1128/MCB.05808-11.
38. **Roy R, Chun J, Powell SN.** 2012. BRCA1 and BRCA2: different roles in a common pathway of genome protection. Nat Rev Cancer **12:**68–78. http://dx.doi.org/10.1038/nrc3181.
39. **Liu S, Chu J, Yucer N, Leng M, Wang SY, Chen BP, Hittelman WN, Wang Y.** 2011. RING finger and WD repeat domain 3 (RFWD3) associates with replication protein A (RPA) and facilitates RPA-mediated DNA damage response. J Biol Chem **286:**22314–22322. http://dx.doi.org/10.1074/jbc.M111.222802.
40. **Tan NGS, Ardley HC, Rose SA, Leek JP, Markham AF, Robinson PA.** 2000. Characterisation of the human and mouse orthologues of the Drosophila ariadne gene. Cytogenet Cell Genet **90:**242–245. http://dx.doi.org/10.1159/000056780.
41. **Li Z, Musich PR, Zou Y.** 2011. Differential DNA damage responses in p53 proficient and deficient cells: cisplatin-induced nuclear import of XPA is independent of ATR checkpoint in p53-deficient lung cancer cells. Int J Biochem Mol Biol **2:**138–145.
42. **Medema RH, Macurek L.** 2012. Checkpoint control and cancer. Oncogene **31:**2601–2613. http://dx.doi.org/10.1038/onc.2011.451.
43. **Kumar V, Sabatini D, Pandey P, Gingras AC, Majumder PK, Kumar M, Yuan ZM, Carmichael G, Weichselbaum R, Sonenberg N, Kufe D, Kharbanda S.** 2000. Regulation of the rapamycin and FKBP-target 1/mammalian target of rapamycin and cap-dependent initiation of translation by the c-Abl protein-tyrosine kinase. J Biol Chem **275:**10779–10787. http://dx.doi.org/10.1074/jbc.275.15.10779.
44. **Tan NG, Ardley HC, Scott GB, Rose SA, Markham AF, Robinson PA.** 2003. Human homologue of ariadne promotes the ubiquitylation of translation initiation factor 4E homologous protein, 4EHP. FEBS Lett **554:**501–504. http://dx.doi.org/10.1016/S0014-5793(03)01235-3.
45. **Matsumoto A, Onoyama I, Sunabori T, Kageyama R, Okano H, Nakayama KI.** 2011. Fbxw7-dependent degradation of Notch is required for control of "stemness" and neuronal-glial differentiation in neural stem cells. J Biol Chem **286:**13754–13764. http://dx.doi.org/10.1074/jbc.M110.194936.
46. **Welcker M, Clurman BE.** 2008. FBW7 ubiquitin ligase: a tumour suppressor at the crossroads of cell division, growth and differentiation. Nat Rev Cancer **8:**83–93. http://dx.doi.org/10.1038/nrc2290.
47. **Yi Z, Yi T, Wu Z.** 2006. cDNA cloning, characterization and expression analysis of DTX2, a human WWE and RING-finger gene, in human embryos. DNA Seq **17:**175–180.
48. **Balut CM, Loch CM, Devor DC.** 2011. Role of ubiquitylation and USP8-dependent deubiquitylation in the endocytosis and lysosomal targeting of plasma membrane KCa3.1. FASEB J **25:**3938–3948. http://dx.doi.org/10.1096/fj.11-187005.
49. **Kuroda TS, Fukuda M, Ariga H, Mikoshiba K.** 2002. The Slp homology domain of synaptotagmin-like proteins 1-4 and Slac2 functions as a novel Rab27A binding domain. J Biol Chem **277:**9212–9218. http://dx.doi.org/10.1074/jbc.M112414200.
50. **Yamamoto H, Koga H, Katoh Y, Takahashi S, Nakayama K, Shin HW.** 2010. Functional cross-talk between Rab14 and Rab4 through a dual effector, RUFY1/Rabip4. Mol Biol Cell **21:**2746–2755. http://dx.doi.org/10.1091/mbc.E10-01-0074.
51. **Larsen DH, Poinsignon C, Gudjonsson T, Dinant C, Payne MR, Hari**

FJ, Rendtlew Danielsen JM, Menard P, Sand JC, Stucki M, Lukas C, Bartek J, Andersen JS, Lukas J. 2010. The chromatin-remodeling factor CHD4 coordinates signaling and repair after DNA damage. J Cell Biol **190:**731–740. http://dx.doi.org/10.1083/jcb.200912135.

52. **Nakayama EE, Shioda T.** 2010. Anti-retroviral activity of TRIM5 alpha. Rev Med Virol **20:**77–92. http://dx.doi.org/10.1002/rmv.637.
53. **Okumura F, Matsuzaki M, Nakatsukasa K, Kamura T.** 2012. The role of elongin BC-containing ubiquitin ligases. Front Oncol **2:**10. http://dx.doi.org/10.3389/fonc.2012.00010.
54. **Cencic R, Hall DR, Robert F, Du Y, Min J, Li L, Qui M, Lewis I, Kurtkaya S, Dingledine R, Fu H, Kozakov D, Vajda S, Pelletier J.** 2011. Reversing chemoresistance by small molecule inhibition of the translation initiation complex eIF4F. Proc Natl Acad Sci U S A **108:**1046–1051. http://dx.doi.org/10.1073/pnas.1011477108.
55. **Shamji AF, Nghiem P, Schreiber SL.** 2003. Integration of growth factor and nutrient signaling: implications for cancer biology. Mol Cell **12:**271–280. http://dx.doi.org/10.1016/j.molcel.2003.08.016.
56. **Clarke R, Cook KL, Hu R, Facey CO, Tavassoly I, Schwartz JL, Baumann WT, Tyson JJ, Xuan J, Wang Y, Warri A, Shajahan AN.** 2012. Endoplasmic reticulum stress, the unfolded protein response, autophagy, and the integrated regulation of breast cancer cell fate. Cancer Res **72:**1321–1331. http://dx.doi.org/10.1158/1538-7445.AM2012-1321.
57. **Morita M, Ler LW, Fabian MR, Siddiqui N, Mullin M, Henderson VC, Alain T, Fonseca BD, Karashchuk G, Bennett CF, Kabuta T, Higashi S, Larsson O, Topisirovic I, Smith RJ, Gingras AC, Sonenberg N.** 2012. A novel 4EHP-GIGYF2 translational repressor complex is essential for mammalian development. Mol Cell Biol **32:**3585–3593. http://dx.doi.org/10.1128/MCB.00455-12.
58. **Sonenberg N, Gingras AC.** 1998. The mRNA 5′ cap-binding protein eIF4E and control of cell growth. Curr Opin Cell Biol **10:**268–275. http://dx.doi.org/10.1016/S0955-0674(98)80150-6.
59. **Cho PF, Poulin F, Cho-Park YA, Cho-Park IB, Chicoine JD, Lasko P, Sonenberg N.** 2005. A new paradigm for translational control: inhibition via 5′-3′ mRNA tethering by Bicoid and the eIF4E cognate 4EHP. Cell **121:**411–423. http://dx.doi.org/10.1016/j.cell.2005.02.024.
60. **Lasko P.** 2011. Posttranscriptional regulation in Drosophila oocytes and early embryos. Wiley Interdiscip Rev RNA **2:**408–416. http://dx.doi.org/10.1002/wrna.70.
61. **Bensimon A, Schmidt A, Ziv Y, Elkon R, Wang SY, Chen DJ, Aebersold R, Shiloh Y.** 2010. ATM-dependent and -independent dynamics of the nuclear phosphoproteome after DNA damage. Sci Signal **3:**rs3. http://dx.doi.org/10.1126/scisignal.2001034.
62. **Bennetzen MV, Larsen DH, Bunkenborg J, Bartek J, Lukas J, Andersen JS.** 2010. Site-specific phosphorylation dynamics of the nuclear proteome during the DNA damage response. Mol Cell Proteomics **9:**1314–1323. http://dx.doi.org/10.1074/mcp.M900616-MCP200.
63. **Joshi B, Cameron A, Jagus R.** 2004. Characterization of mammalian eIF4E-family members. Eur J Biochem **271:**2189–2203. http://dx.doi.org/10.1111/j.1432-1033.2004.04149.x.
64. **Wiseman RL, Balch WE.** 2005. A new pharmacology—drugging stressed folding pathways. Trends Mol Med **11:**347–350. http://dx.doi.org/10.1016/j.molmed.2005.06.011.